Eur. Phys. J. Plus (2020) 135:105
https://doi.org/10.1140/epjp/s13360-020-00162-9

THE EUROPEAN PHYSICAL JOURNAL PLUS

Regular Article

Benchmarking of M*ANCINTA*P 2.0, a parallel high-performance tool for neutron activation analysis in complex 4D scenarios

Gabriele Firpo[a], **Michele Frignani, Carlo Maria Viberti**

Ansaldo Nucleare SpA, Corso Perrone 25, 16151 Genoa, Italy

Received: 10 May 2019 / Accepted: 11 November 2019 / Published online: 23 January 2020

Abstract M*ANCINTA*P is a parallel computational tool developed and maintained by Ansaldo Nucleare since 2011 to perform 4D neutron transport, activation and time-resolved dose-rate calculations in complex geometries for CPU-intensive applications. M*ANCINTA*P creates an automated link between the 3D radiation transport code MCNP5—which is used to evaluate both the neutron fluxes for activation calculations and the resulting secondary photon dose rates—and the zero-dimensional activation code Anita2000 by handling crucial processes such as data exchange, determination of material mixtures and generation of cumulative probability distributions. Ansaldo Nucleare recently developed a new version of the tool, named M*ANCINTA*P 2.0. A brief description of the computational tool is given here, with particular emphasis on the key technical choices underlying the project. The main enhancement is here highlighted with respect to the former version, and the results of a benchmarking campaign of M*ANCINTA*P 2.0 against the Monte Carlo code FLUKA are described for two test cases.

1 Introduction

M*ANCINTA*P [1, 2] is a computer program developed by the Radiation Analysis group at Ansaldo Nucleare to bridge the gap between the three-dimensional radiation transport code MCNP5 [3] and the zero-dimensional activation code Anita2000 [4, 5]—solver of the Bateman Equations. The purpose of this tool is to exploit the capabilities of both codes in order to provide the user with a complete and automatic program for the 4D analysis of neutron activation scenarios in complex geometries (e.g., fusion and fission reactors, particle accelerators, etc.).

When performing a calculation with the M*ANCINTA*P program, all the neutron and photon transport calculations are performed by the MCNP5 v. 1.6 code, and all the activation calculations—i.e., solution of the Bateman equations—are performed by the Anita2000 kernel. M*ANCINTA*P provides an interface between the two codes by handling pre- and post-processing and communication tasks such as data exchange, determination of material mixtures and translation of the activation photon source distributions from the Anita2000 to the MCNP5 format. Both underlying codes are stretched by M*ANCINTA*P beyond their

[a] e-mail: Gabriele.Firpo@ann.ansaldoenergia.com

classical domain of usage: For instance, the mesh tally values calculated by MCNP5 are directly used for subsequent calculations without formal statistical reliability, which should be ensured by other means [1].

A first version of the M*ANCINTA*P tool, named M*ANCINTA*P 1.0 in the following, was developed from 2011 to 2013 [1, 2], while recently a new version of the tool, named M*ANCINTA*P 2.0 in the following, was developed in order to fix minor bugs and to enhance the applicability range of the tool in the framework of the neutron activation analysis.

The aim of the present paper is to describe the M*ANCINTA*P 2.0 capabilities as well as to present the results of a dedicated benchmarking campaign against the Monte Carlo FLUKA code [6, 7].

This paper is organized as follows: an overview of the M*ANCINTA*P tool; the main enhancement of the actual version M*ANCINTA*P 2.0 as well as the details on its functionalities are reported in Sect. 2; a description of the performed benchmark tests against the FLUKA code and a discussion of their results follow in Sect. 3. The main conclusions are summarized in Sect. 4.

2 M*ANCINTA*P system description

The description of the M*ANCINTA*P general approach, the description of the main differences between M*ANCINTA*P 1.0 and M*ANCINTA*P 2.0 and details on M*ANCINTA*P 2.0 functionalities are reported in Sects. 2.1, 2.2 and 2.3, respectively.

2.1 The M*ANCINTA*P approach

M*ANCINTA*P employs a Rigorous Two-Step (R2S) methodology [8]. As the name suggests, the evaluation of nuclear responses from a neutron activation process is divided into two main steps:

1. A neutron transport calculation is performed in order to evaluate the neutron fluxes and spectra in a series of regions of interest, of variable size and material composition. A neutron activation code is then used to predict, from the evaluated neutron flux, the radionuclide inventory and the corresponding activation photon source spectra in each location for all the cooling times of interest;
2. The activation photon distributions are then sampled in a second, photon-only transport calculation, in order to determine the activation photon fluxes and spectra and other derived quantities in the spatial regions of interest (e.g., radiation dose maps).

The R2S method has proven to be the most accurate way of calculating almost any nuclear quantity involving neutron activation, since it makes no appreciable approximation with regard to neutron transport, nuclear activation and subsequent photon transport [8].

Within the M*ANCINTA*P scheme, the neutron and photon radiation transport calculations are performed as standard MCNP5 runs and can thus be incorporated into the chain of calculations through a simple, dedicated UNIX shell script. On the other hand, the link between the two calculations—including the use of an activation inventory code—is a delicate process which involves the exchange and correct management of a large quantity of data. The goal of the M*ANCINTA*P kernel is precisely to tackle this calculation stage, by seamlessly managing all data exchanges between the transportation calculations and the Anita2000 kernel.

2.2 M*ANCINTA*P 1.0 vs M*ANCINTA*P 2.0

The main scope of the M*ANCINTA*P 1.0 code [1, 2] was to perform entirely the R2S analysis described above. This means that the whished outcome was the determination of the nuclear responses due to the activation photons, which is needed; for instance, in case radiation maps are to be evaluated inside nuclear facilities in shutdown conditions, close to and/or far from the activated components. The detailed information of the activated components at the end of the first step—*i.e.*, the nuclide inventories and the corresponding photon spectra—was not stored nor saved, since this information was used as interface and volatile (through the RAM) data between the neutron transport and the neutron activation codes.

M*ANCINTA*P 1.0 already included some computational optimization facts like the minimization of disk access operations through the extensive use of *named pipes* [9] and a straightforward approach to the parallel execution through the message passing interface (MPI) [10], in order to manage massive *high-performance computing* (HPC) analyses. This was achieved through a dedicated, parallel-memory management architecture, bypassing any disk access operation and using an effective parallel computing approach in order to achieve quasi-linear speedup. The results of some benchmark activities as well as details on the scalability analysis of the parallel version of M*ANCINTA*P 1.0 are discussed in [11].

The main motivation that recently brought to the development of a new version of M*ANCINTA*P was the need to collect also the information on the activated component at the end of the first step of the R2S approach, in order to perform nuclear waste classification analyses, while preserving all the HPC capabilities of the previous version. Moreover, M*ANCINTA*P 2.0 includes also the capability to propagate the statistical uncertainties on the neutron flux: The second step of the R2S approach can be performed considering the average neutron flux values as well as considering an arbitrary number of statistical standard deviations on them.

2.3 Details on M*ANCINTA*P 2.0 functionalities

The full flowchart of the algorithm used by M*ANCINTA*P 2.0 is shown in Fig. 1. The M*ANCINTA*P 2.0 kernel takes as input the results of the first neutron transport calculation and yields the photon source distributions for all regions and cooling times of interest. An irradiation history, composed of multiple irradiation times (together with related power fractions) and intermediate dwell times, as well as the cooling times at which photon sources need to be calculated, is specified as input parameters. The calculation process, divided into three main steps, is outlined in the rest of this section, along with the main reasons behind the principal technical choices made.

2.3.1 Input data processing

The starting point of the M*ANCINTA*P kernel is the space and energy distribution of the neutron flux, as properly obtained in the first MCNP5 run. One or more *mesh tallies* [3] shall be defined to cover all the regions of interest for the activation calculation, allowing MCNP5 to record and store flux distributions. Many different meshes—with arbitrary geometry (rectangular, cylindrical or spherical), dimensions and energy bins—can be used at the same time to flexibly and accurately capture details of different sizes and shapes; they will be treated and combined by the M*ANCINTA*P 2.0 kernel in subsequent calculations [2].

Once the neutron flux calculation is carried out, only the binary output ("*runtpe*") file produced by MCNP5 is used as an input by M*ANCINTA*P 2.0, providing complete access

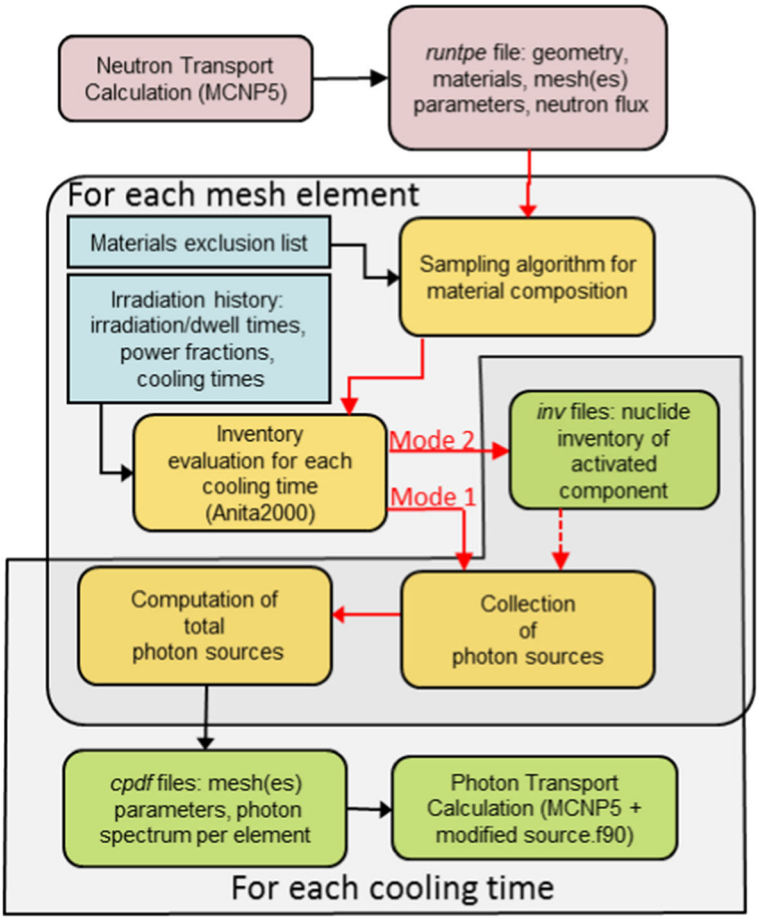

Fig. 1 Flowchart of the M*ANCINTA*P 2.0 system. Parallel operations are outlined by multiple red arrows. The blocks with an orange background represent the M*ANCINTA*P 2.0 kernel

to all the model information (mesh, combinatorial geometry, materials, fluxes, etc.) needed for a precise evaluation of critical quantities (e.g., material mixture in each mesh cell). The choice of using a direct access binary file was preferred to an ASCII file in terms of performances, even if restricts somewhat the portability of the code. In addition, the above listed information cannot be easily obtained from other output files produced by an unmodified version of MCNP5. A slight loss of portability during this stage was deemed acceptable, since a guiding principle in the development of this tool has been to avoid modifying the MCNP5 source code beyond what is recommended by its user manual, thus avoiding any potential impact on its results—which would require a thorough re-qualification process.

2.3.2 Computation of materials, nuclide inventories and activation photon spectra

Once the *runtpe* file of the neutron calculation is available, the M*ANCINTA*P 2.0 kernel is used to automatically calculate the resulting photon sources for a given irradiation history and for all relevant cooling times. From this point on, the execution of the code is completely

parallel and can be run on any number of processes without limitation. All code was written in C++, with some dedicated FORTRAN routines acting as wrappers/interfaces between the main code and the specific MCNP5 and Anita2000 source codes,[1] while the parallelization scheme was based on the standard MPI protocol.

The nature of the problem allows for an *embarrassingly parallel* treatment of almost all calculations, since any mesh element can be treated independently from the neighboring ones. Moreover, the implementation scheme was designed to further minimize all communications between processes during the initial data-collection and material-determination phases. The logical steps, each of the parallel processes undertakes, are then exactly the same, with no true master/slave distinction.[2]

When the program starts, each process opens the *runtpe* file and reads the general problem and mesh geometry information. Each process then selects—using a simple mathematical formula and with no need of inter-process communication—a subset of mesh elements, of which it will be solely in charge.

The next step is the determination of the material composition and effective density of the mixture of materials present in each mesh cell. In fact, simply considering one material for each mesh cell (either the most represented or the one at the center) would be too crude an approximation and would impose an unnecessary constraint on the maximum mesh cell size. The complete knowledge coming from an unrestricted access to the *runtpe* file allows performing this step with sub-mesh precision. A simple Monte Carlo process was used: The cell is uniformly sampled and the material at each sample point is used to build a new homogenized material, through a volume-based weighted average of materials and densities. The approach was considered a good compromise between a fast execution and the preservation of the total mass of each material: The latter is only achieved asymptotically, but in practise very good results can be obtained with only few sample points. Conserving the total mass of the materials is a very important feature, preventing not only skewing effects on local quantities, but also errors in integral ones, such as total activation source or average gamma dose rate. Note that should any material be irrelevant to the activation problem, it can be excluded from the following computational steps by listing it in the M*ANCINTA*P 2.0 input file.

Once material mixtures and effective densities are determined, each process retrieves from the *runtpe* file, the neutron flux and spectrum as calculated by MCNP5 for its mesh cells and uses it to calculate the gamma sources via a call to the Anita2000 activation code. If performed by a mere program execution, this operation would require a large amount of data to be written on the hard-drive, thus affecting the performance, especially in parallel runs with large meshes. Now, two modes are available as options in the M*ANCINTA*P 2.0 input file, depending on the scope of the analysis: the evaluation of nuclear response of activation photons only (Mode 1) or, exclusively or also in addition, the evaluation of activation information of the activated components (Mode 2).

In Mode 1, in order to completely eliminate all disk access, while still avoiding any modification to the Anita2000 source code, all the I/O operations between MCNP5 and Anita2000 are performed through UNIX *named pipes* instead of actual files, thus granting a significant speedup, as all disk-access operations are replaced by RAM-access ones. As a consequence, intermediate files are not stored, which can hinder quality check operations on

[1] The class structure was designed with a modular pattern, with general and dedicated classes handling the main process and the I/O operations, respectively, with the goal of eventually allowing a multiple choice of activation kernels and/or transport codes.

[2] Except for user I/O and logging operations.

the activation calculations. The second step of the R2S approach is then ready to be executed, as described in the following subsection.

In Mode 2, apart from executing the same functionalities of Mode 1, M*ANCINTA*P 2.0 writes also all the intermediate files—i.e., the complete set of ASCII Anita2000 output files for each mesh element at each cooling time—to the hard-drive, albeit with a performance overhead. This is done easily because of the completely interchangeable nature of *named pipes* and normal files [9]. Moreover, a single ASCII summary file—called *inv*—listing the nuclide inventory for each mesh element at each cooling time is also written to disk. Thanks to this functionality, a comprehensive analysis of the nuclide inventories of the activated components at each cooling time can be performed.

The user is warned by the fact that a huge amount of data and corresponding disk space can arise in Mode 2.

In both Mode 1 and Mode 2, the user can tell M*ANCINTA*P 2.0 to perform optionally all the operations described above considering not only the mean neutron flux values evaluated inside each mesh cell in the first step of the R2S approach, but also the mean neutron flux values plus and minus an arbitrary number of statistical standard deviations. Hence, the statistical uncertainties related to the first step of the R2S approach are propagated on both the subsequent photon nuclear response and nuclide inventory analyses. This approach is performed bin-by-bin with the statistical uncertainties that MCNP provides for the neutron flux in each energy bin. It is emphasized that by this way the results of calculations depend on binning choice, because the statistical uncertainty of the bin-by-bin flux is typically higher in bins with smaller size. Even in case any algorithm made the statistical errors independent to binning choice, the overall statistics of the neutronic MCNP calculation would be every time-dependent on the number of histories run and/or on the used variance reduction techniques (if any). It is user's responsibility to perform optimization of statistics of the neutronic MCNP run.

2.3.3 Merging of probability distribution functions

The capability described hereafter is provided to cope with the case where the second step of the R2S approach is needed. With the information on the photon spectra and source strengths stored in memory at the end of the first step in both Mode 1 and Mode 2, the master process of M*ANCINTA*P 2.0 retrieves all partial data from all processes and builds cumulative probability distribution functions (*cpdf*), one for each cooling time, representing the space and energy distribution of decay photon sources. When needed, the *cpdf* files considering the addition of an arbitrary number of statistical standard deviations on the neutron flux are created also. These files are then read by a suitably modified version of MCNP5 for the final—sequential or parallel—photon transport runs. Sampling these files only requires implementing a very simple *source.f90* subroutine [3], as allowed by the MCNP5 developers, without representing a breach of MCNP5's code qualification.

While the use of an MCNP5 *sdef* card [3] would be an even safer way, a complete description of photon sources would be impossible for large problems, due to intrinsic limitations of the card extension, thus requiring the execution of multiple partial runs and the combination of their results.

All source particles are produced with a unitary weight, thus allowing maximum flexibility in the use of variance reduction techniques in subsequent photon transport calculations. Complete portability is furthermore guaranteed by plain ASCII format.

The M*ANCINTA*P 2.0 kernel—plus the modified version of MCNP5 capable of reading *cpdf* files—can be considered as the complete M*ANCINTA*P system.

Table 1 Material composition of SS316LN

Element	Mass fraction
Fe	6.71E−01
Cr	1.85E−01
Ni	1.13E−01
Mn	2.00E−02
Si	1.00E−02
P	4.50E−04
S	3.00E−04
C	3.00E−04

3 Benchmarking of M*ANCINTA*P 2.0

Benchmarking of the M*ANCINTA*P 2.0 system is performed against the FLUKA Monte Carlo code [6,7]. The used FLUKA version is 2011.2c.5.3. Two benchmarks are performed considering:

- *#1*—A $1 \times 1 \times 1$ cm^3 void source cube is set as the neutron source, and the activation analysis is evaluated on two $1 \times 1 \times 1$ cm^3 cubes made by pure Cobalt (*#1.1*) or steel (*#1.2*). Both the nuclear response (spatial distribution of photon dose rates) and the nuclide inventory (the latter only for *Benchmark 1.2*) are compared;
- *#2*—A $1 \times 1 \times 1$ cm^3 void source cube is set as the neutron source; a steel slab, with a cylindrical hole, is placed nearby and a $1 \times 1 \times 1$ cm^3 cube made by pure Cobalt, not in the line of sight of the hole, is placed behind the slab. The nuclear response (spatial distribution of photon dose rate) created by both the steel slab and the cobalt cube is compared;

In all the cases, the typical material composition of SS316LN, reported in Table 1, is used as reference for the steel component; its density is set to 7.8 g/cm^3. The material density of the pure Cobalt is set to 8.9 g/cm^3.

The default nuclear library dataset, based on the most important evaluations (ENDF/B, JEF, JENDL, etc.) are used with FLUKA. In M*ANCINTA*P, the neutron ENDF/B-VI and EAF99 library datasets are used for the MCNP5 and Anita2000 codes, respectively, in the first step of the R2S approach, whereas the photon ENDF/B-VI library dataset and the ICRP 74 H*(10) photon flux to dose conversion factors are used to evaluate the activation photon dose rates in the last step of the R2S approach.[3]

The detailed descriptions of the geometries and irradiation histories setup, as well as the calculation results, are reported in Sects. 3.2 and 3.3 for *#1* and *#2*, respectively. Previously, the main differences between the neutron activation analyses as performed by the two codes are browsed hereafter; this description is useful to better understand the benchmark results.

3.1 Comparison between FLUKA and MANCINTAP neutron activation approaches

FLUKA can perform the activation analysis both in the so-called semi-analytical and semi-analogue modes. In the "semi-analytical" mode, FLUKA evaluates the nuclide inventory at the desired cooling time(s) by computing the initial residual nuclei via Monte Carlo method and by computing the decay/build-up of the residual nuclei via the solution of Bateman

[3] Note that the MCNP5 v. 1.4 was used for the benchmark activities presented in this paper. That's why the corresponding default ENDF/B-VI dataset libraries were used.

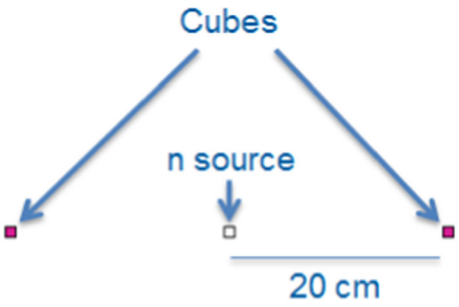

Fig. 2 System configuration for the Benchmark 1

Equations; a database of photon decay emissions is used to simulate the activation photon source and spectra, which are transported with Monte Carlo method to get the nuclear response of the activation photons. Conversely, in the "semi-analogue" mode, FLUKA applies the pure Monte Carlo method to perform the evaluation of both the nuclide inventories and the nuclear response of the activation photons. Since the "semi-analytical" mode is closer to the implementation of the R2S approach of M*ANCINTA*P than the "semi-analogue" mode, only the "semi-analytical" mode is considered in FLUKA for the present benchmark.

The main differences between the "semi-analytical" mode of FLUKA and the R2S implementation of M*ANCINTA*P can be defined as follows. Considering the first step of the R2S approach, in FLUKA the residual nuclei are evaluated via Monte Carlo method, hence by pointwise spatial resolution; conversely, in M*ANCINTA*P the residual nuclei are analytically evaluated considering the neutron flux averaged in each mesh cell, hence the spatial resolution is user-dependent. Considering instead the second step of the R2S approach, in FLUKA the activation photons have a realistic line energy spectrum shape; conversely, in M*ANCINTA*P the photons are binned in 14 energy groups—as inherited from the Anita2000 code.

Summarizing, the FLUKA approach can be considered more accurate than the M*ANCINTA*P one. Anyway, when dealing with complicated and/or extended geometries, the pointwise approach of FLUKA can require a significant computing time to get acceptable statistics. In this case and, in general, in all the cases where the averaging approach of M*ANCINTA*P is reliable, M*ANCINTA*P can be considered as an efficient alternative to FLUKA.

3.2 Benchmark #1

In the first benchmark, a $1 \times 1 \times 1$ cm^3 void source cube is set as the neutron source, and the activation analysis is evaluated on two $1 \times 1 \times 1$ cm^3 cubes made by pure Cobalt (*#1.1*) or steel (*#1.2*), symmetrically placed 20 cm far from the source. The geometry of the system is depicted in Fig. 2.

The typical fusion neutron spectrum (~ 14 MeV) is defined as an isotropic source in the source cube; the irradiation time is set to 2 h, with constant intensity equal to 1e12 n/s. A single cooling time at 1 month after irradiation is considered as time instant for the neutron activation analysis.

As an example, the results of both the spatial neutron flux and activation photon dose rate distributions as obtained with FLUKA in *#1.1* are reported in Figs. 3 and 4, respectively.

Qualitatively, as expected, the same behavior was obtained also in *#1.2* as well as in case of use of M*ANCINTA*P, where the neutron meshes are defined as a single mesh cell coincident with the cubes. The results of a quantitative analysis follow hereafter.

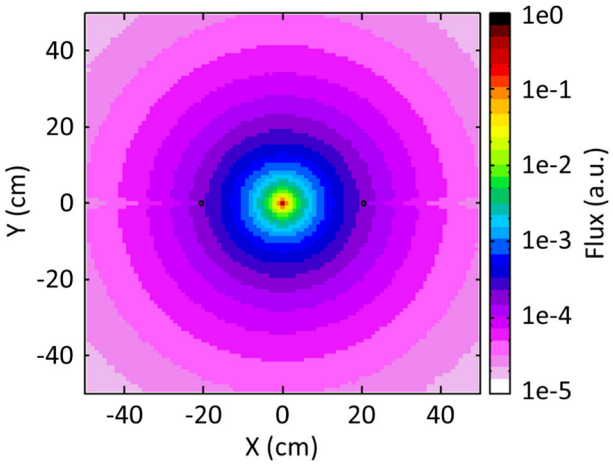

Fig. 3 Spatial distribution of the neutron flux

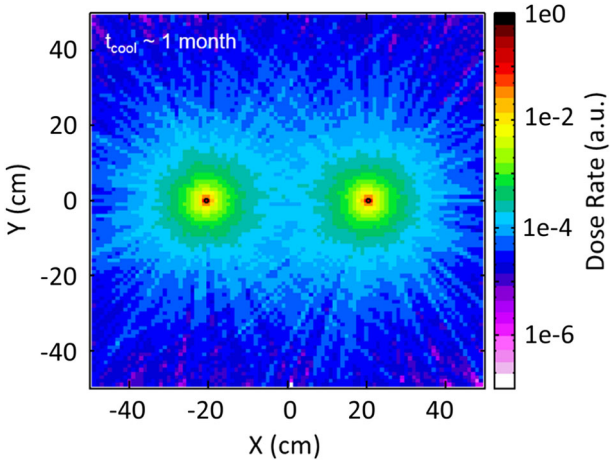

Fig. 4 Spatial distribution of the activation photon dose rate at 1 month after irradiation

#1.1—Pure cobalt cubes

The quantitative comparison of the activation photon dose rate values between FLUKA and M*ANCINTA*P was performed defining in both the codes a rectangular photon dose rate mesh with spatial resolution equal to 1 cm on all directions. The dose rate values along the line depicted in Fig. 5 are plotted in Fig. 6.

The results show a very good agreement between the codes, since the dose rate values differ no more than ~4%.

#1.2—Steel cubes

The same approach used for *#1.1* was used also for the quantitative comparison of the activation photon dose rates in case of steel cubes.

The dose rate values along the line depicted in Fig. 5 were extracted and plotted as shown in Fig. 7. The agreement in this case was not as good as in case of the pure Cobalt cubes,

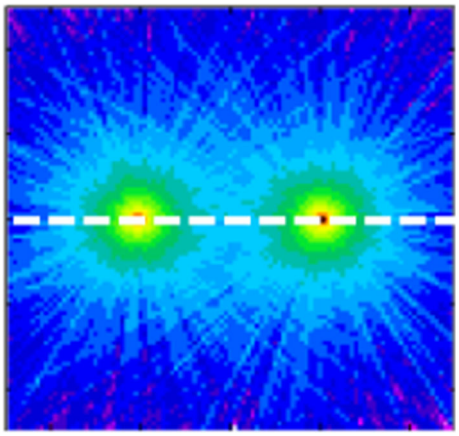

Fig. 5 White line defines the path along which the dose rate is quantitatively compared between FLUKA and M*ANCINTAP*

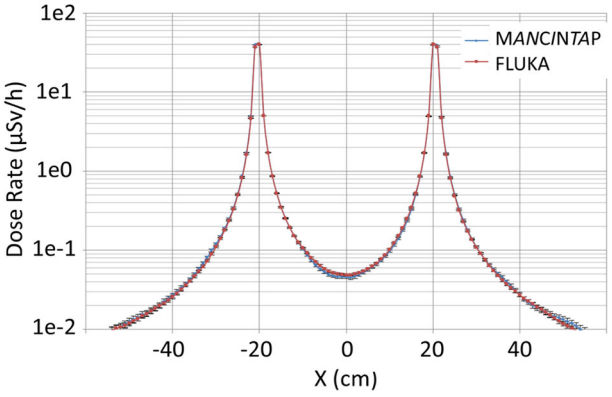

Fig. 6 Comparison between the distribution of the activation photon dose rate of the pure Cobalt cubes along the line defined in Fig. 5

since the dose rate values differ, for example, by ~40% just at the position of the activated cubes.

This issue was further investigated considering that, in principle, the discrepancies can arise at any step of the R2S approach, that is:

- First step: neutron flux and residual nuclei estimation—any difference on transport and activation neutron libraries used in the two codes can bring to significant difference in the nuclide inventories at the considered cooling time;
- Second step: transport of the activation photons—even in case of equivalent nuclide inventory, the energy discretization of the corresponding photon source spectra can bring to significant differences on the spatial dose rates at the considered cooling time.

A quantitative comparison between the residual nuclei inventories (in terms of their activities in Bq) obtained by FLUKA and M*ANCINTAP* at the considered cooling time, here shown in Table 2, brought to the conclusion that the difference on the photon dose rate distributions is not due to the first step of the R2S approach in M*ANCINTAP*: in fact, a very good agreement (no more than few percent difference) on the dominant nuclei is observed.

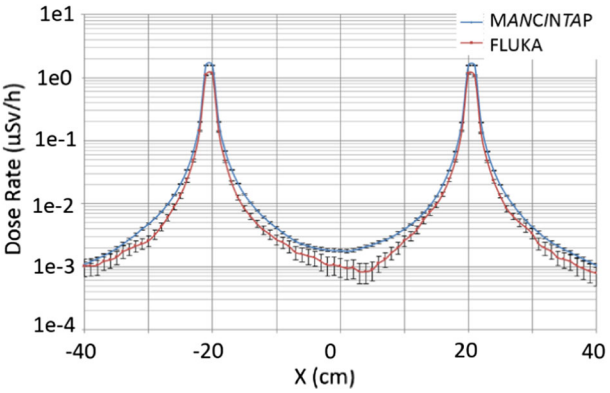

Fig. 7 Comparison between the distribution of the activation photon dose rate of the steel cubes along the line defined in Fig. 5

Table 2 Comparison between the nuclide inventories of the steel cubes at 1 month after irradiation as obtained by FLUKA and M*ANCINTAP*. The statistical uncertainties on the activity values are below 5% in all the cases

Nuclide	ManCiNtaP activity [Bq]	FLUKA activity [Bq]	Difference (%)
51Cr	1.13E+03	1.16E+03	− 1.98
55Fe	2.54E+02	2.60E+02	− 2.18
58Co	1.67E+02	1.63E+02	2.65
57Co	1.38E+02	1.52E+02	− 9.22
54Mn	6.65E+01	6.35E+01	4.87
49 V	1.54E+01	1.14E+01	35.50
32P	1.59E+00	1.27E+00	25.48
60Co	1.47E+00	1.29E+00	13.83
Total	1.78E+03	1.81E+03	− 1.65

Significant differences arise only for negligible nuclei, having activities less than 1% of the total.

On the contrary, the comparison between the activation photon source spectra obtained by FLUKA and M*ANCINTAP* at the considered cooling time, here shown in Fig. 8, lead to the conclusion that the energy grouping (binning) approach of M*ANCINTAP* versus the line spectrum approach of FLUKA could in principle explain the observed difference on the photon dose rate distributions.

The simpler nuclide inventory of *#1.1*, realistically dominated by the activated Cobalt-60 isotope only, made this issue not to appear there.

3.3 Benchmark #2

In the second benchmark, a $1 \times 1 \times 1$ cm^3 void source cube is again set as the neutron source; a $40 \times 40 \times 2$ cm^3 steel slab, with a cylindrical hole with radius 1 cm, is placed at 10 cm from the source and a $1 \times 1 \times 1$ cm^3 cube made by pure Cobalt, not in the line of sight of the hole (~5 cm from the hole axis), is placed behind the slab at 10 cm from it. The geometry of the system is depicted in Fig. 9.

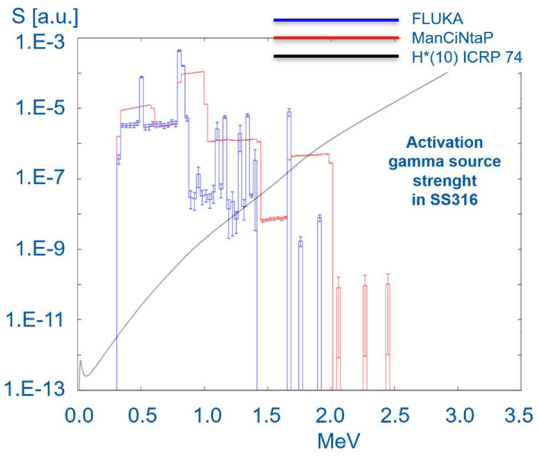

Fig. 8 Normalized activation source spectra of the steel cubes at 1 month after irradiation as obtained by FLUKA (in blue) and M*ANCINTA*P (in red)

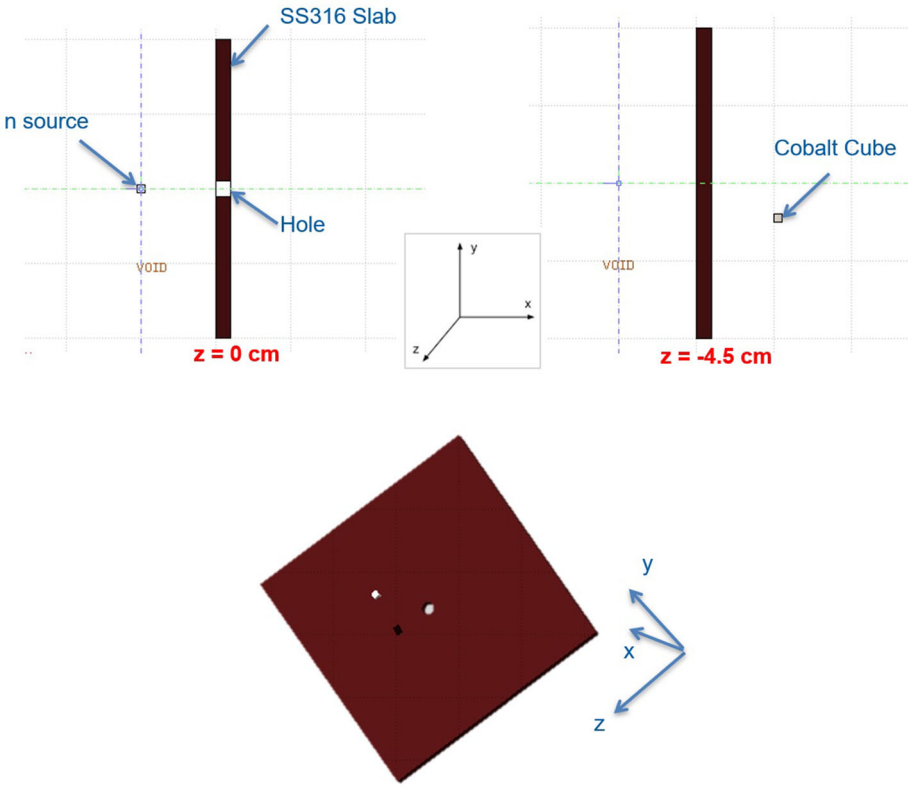

Fig. 9 System configuration for the Benchmark 2

Again, the typical fusion neutron spectrum (~ 14 MeV) is defined as an isotropic source in the source cube; the irradiation time is set to 2 h, with constant intensity equal to 1e12 n/s. Two cooling times (1 s and 1 month after irradiation) are considered as time instants for the neutron activation analysis.

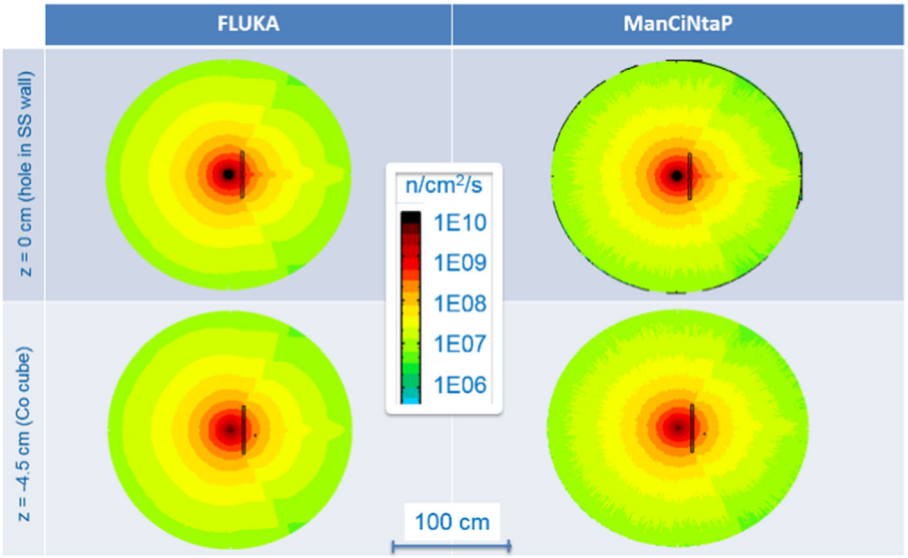

Fig. 10 Spatial distributions of the neutron flux on the plane of the hole in steel slab (on top) and on the plane of the cobalt cube (on bottom) as obtained by FLUKA and M*ANCINTA*P

In M*ANCINTA*P, the steel slab and the cobalt cube where tallied with a $40 \times 40 \times 2$ and a $1 \times 1 \times 1$ rectangular neutron mesh elements, respectively—hence, the neutron flux spatial resolution was again set to 1 cm on all directions. Since the average neutron mean free path is equal to ~ 4.5 cm in both steel and cobalt materials—as evaluated by MCNP5 calculation—no significant neutron flux gradient occurs inside each mesh cell. This means that the meshes defined in M*ANCINTA*P are fine enough to approximate the pointwise approach of FLUKA.

The qualitative comparison between the results of both the spatial neutron flux and activation photon dose rate distributions as obtained by FLUKA and M*ANCINTA*P is reported in Figs. 10 and 11, respectively.

The quantitative comparison of the activation photon dose rate values between FLUKA and M*ANCINTA*P was performed defining in both the codes a rectangular photon dose rate mesh with spatial resolution equal to 1 cm on all directions. The dose rate values were then extracted along the line depicted in Fig. 12 and plotted in Figs. 13 and 14 at the two considered cooling times, respectively.

Looking at the results, the following conclusions arise:

- At the first cooling time (1 s after irradiation), as expected, the activation dose rate distribution is dominated by the steel of the slab, being more massive than the cobalt cube; again, the disagreement between the results of FLUKA and M*ANCINTA*P (M*ANCINTA*P results are ~ + 15% with respect to FLUKA) can be explained by the difference in the photon energy grouping approach already observed in Benchmark #1;
- At the second cooling time (1 month after irradiation), the activation of the cobalt cube is now dominant because of the longer half-life of Cobalt-60 isotope with respect to the activated isotopes in steel. Again, coherently with what was observed in Benchmark #1, the contribution to the dose rate from the steel is in disagreement between the two codes (M*ANCINTA*P results are ~ + 50% with respect to FLUKA), whereas on the contrary, very good agreement is observed for Cobalt cube.

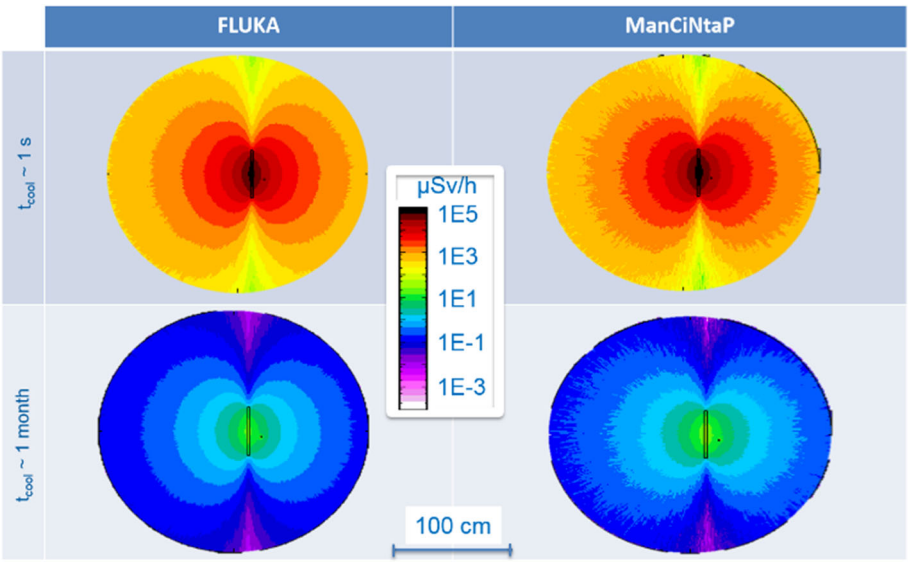

Fig. 11 Spatial distributions of the activation photon dose rates on the plane of the cobalt cube at the considered cooling times as obtained by FLUKA and M*ANCINTA*P

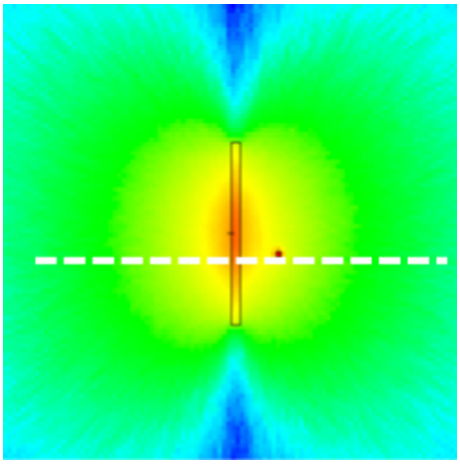

Fig. 12 White line defines the path along which the dose rate is quantitatively compared between FLUKA and M*ANCINTA*P

3.4 Sensitivity analysis with MANCINTAP

Apart from the comparison against FLUKA, the same geometry of Benchmark 2 was used also to perform a sensitivity analysis on the neutron mesh fineness, in order to highlight the importance of the user-dependent choice on the spatial resolution of the neutron mesh in the first step of the R2S approach with M*ANCINTA*P.

The distribution of the activation photon dose rate at 1 month after irradiation along the line defined in Fig. 12 was evaluated with M*ANCINTA*P considering many different neutron meshes on the steel slab (no changes to the neutron mesh on the cobalt cube are applied) with different spatial resolutions, labeled as "N_Y_N_Z_N_X", where N_i is the number of mesh

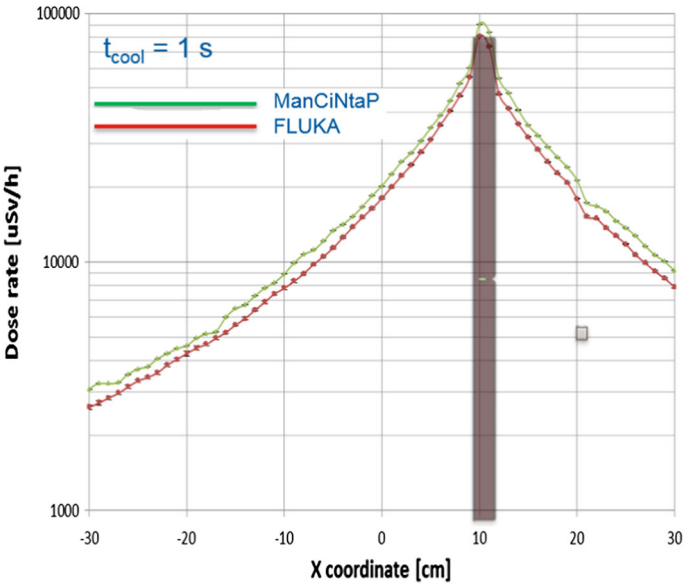

Fig. 13 Comparison between the distribution of the activation photon dose rate at cooling time 1 s along the line defined in Fig. 12

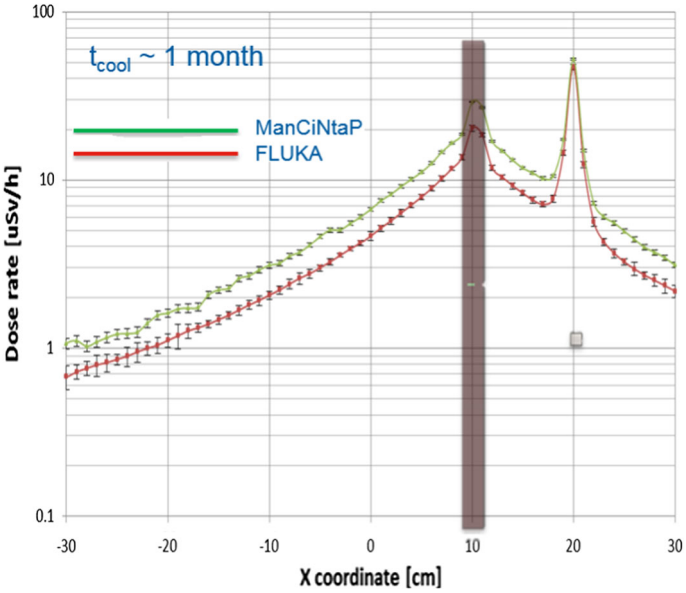

Fig. 14 Comparison between the distribution of the activation photon dose rate at cooling time 1 month along the line defined in Fig. 12

cells in direction i. With good approximation, Y and Z can be considered as the directions perpendicular to the source line of sight, whereas X can be considered as the direction parallel to it.

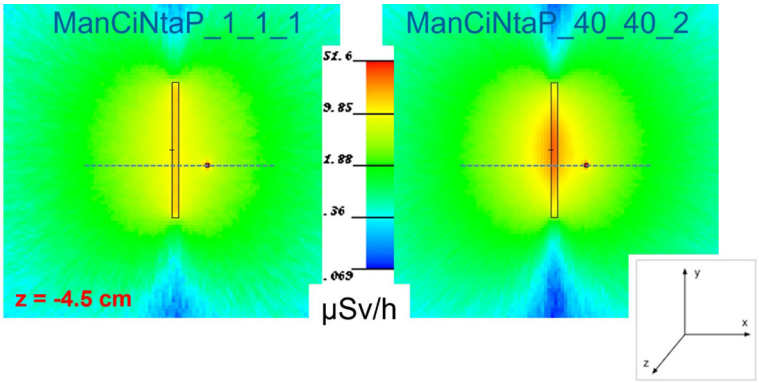

Fig. 15 Spatial distribution of the activation photon dose rates as obtained by M*ANCINTA*P considering different spatial resolution of the neutron mesh

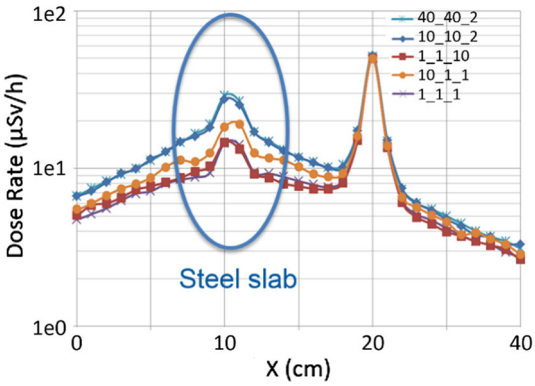

Fig. 16 Comparison between the dose rate distributions along the line defined in Fig. 12, at 1 month after irradiation, considering many neutron mesh spatial resolutions with M*ANCINTA*P

The reference mesh configuration is the finest one already defined for Benchmark #2 (labeled as "40_40_2" in the following); a set of coarser meshes is considered, up to the coarsest one having only one mesh cell (labeled as "1_1_1"). As an example, Fig. 15 shows the significant averaging effect on the spatial distribution of the activation photon dose rate in case of the coarsest and the finest neutron meshes considered in the present sensitivity analysis with M*ANCINTA*P.

Quantitatively, Fig. 16 shows the comparison between the dose rate distributions along the line defined in Fig. 12, at 1 month after irradiation, considering the different mesh spatial resolutions on the steel slab with M*ANCINTA*P. As expected, the peak on the right due to the cobalt cube remains unchanged (since no modifications are applied to the cobalt mesh), whereas significant changes are observed in the region of the steel slab. In particular and as expected, a correlation between the neutron mesh spatial resolution and the neutron mean free path is found:

- As the resolution in the directions perpendicular to the source line of sight becomes coarser than 4 cm—i.e., when N_Y and/or $N_Z < 10$, the dose rate values decrease, coherently with what it is expected by looking at the averaging effect shown in Fig. 15. This can be explained by the fact that as the linear dimension of the mesh cells becomes more than the neutron mean free path, just equal to ~4 cm, the more significant neutron flux gradient inside each mesh cell occurs;

- As the resolution on the directions of the source line of sight becomes coarser—i.e., as N_X decreases, the dose rate values do not significantly change. This can be explained again by that fact that the spatial resolution on this direction in the coarsest considered configuration, equal to 2 cm, is still less than the neutron mean free path, and so no significant neutron flux gradient occurs in the mesh cell.

A *gold rule* can be derived for the M*ANCINTA*P: user the finer is the neutron mesh, the better it is; anyway, since the finer is the mesh, the huger and less efficient is the Monte Carlo calculation also, a good compromise is to set the spatial resolution of the neutron mesh to be no more than the mean free path of neutrons in the material of interest.

4 Conclusions

M*ANCINTA*P, as version 2.0, is a parallel computational tool developed by Ansaldo Nucleare to perform 4D neutron transport, activation and time-resolved dose-rate calculations in very complex geometries for CPU-intensive applications of interest in the fission and fusion fields.

A description of the code and its parallel implementation has been presented. It relies on MCNP5 for the neutron transport and activation photon dose-rate calculations and on Anita2000 for the activation calculations, including the optional evaluation of nuclide inventories for nuclear waste classification purposes.

The main strengths of M*ANCINTA*P 2.0 are the following: (1) it reads neutron fluxes from the MCNP5 *runtpe* binary file, which—though less portable than an ASCII file—contains all the information about the neutron transport run needed for sub-mesh accuracy in evaluating the material compositions; (2) it uses an efficient Monte Carlo material sampling algorithm to determine the material composition at a user-defined level, (3) it relies on processes which enable heavy parallelization, thus increasing performances; (4) communications between MCNP5 and Anita2000 can be all done via named pipes, thus avoiding time consuming I/O operations; (5) activation photon source spectra are produced in ASCII *cpdf* format, thus avoiding all the limitations intrinsic to the use of *sdef* cards; (6) it includes the capability to propagate the statistical uncertainties on the neutron flux throughout all the neutron activation analysis up to the final activation photon nuclear response; (7) it includes the capability to store the detailed information on the nuclide inventories of the activated components, thus letting the nuclear waste classification analysis; (8) it includes the possibility to exclude a user-defined list of material(s) from the activation analysis; (9) it can handle multiple neutron mesh definition in the same system, thus minimizing the number of distinct runs; (10) in principle, it does not critically depend on which particular transport and activation codes are employed—the tool can easily be modified to rely on codes other than MCNP5 and Anita2000.

The results of two benchmarks of M*ANCINTA*P 2.0 against the FLUKA Monte Carlo code have been also presented here. Both the nuclear responses of the activation photon and the nuclide inventories at different cooling times have been evaluated and compared between the two codes, obtaining consistent results. Where some discrepancies have been found, justifications and explanations have been drawn. Moreover, the two benchmarks cover a realistic range of neutron energies, materials and geometries which are important in real-life fusion (but also fission) activation analysis applications, including, but not being limited to, shielding and radiation streaming effects. This can be thus be considered as a demonstration of the M*ANCINTA*P 2.0 code capabilities for a significantly wide range of applications.

References

1. M. Frignani, G. Firpo, S. Frambati, MANCINTAP: a numeric tool for the analysis of neutron induced activations and their radiological effects in complex 3D geometries, in *PHYSOR2010 International Conference*, Pittsburgh, 2010
2. S. Frambati, G. Firpo, M. Frignani, MANCINTAP: time and space dependent neutron activation tool algorithm improvement and analysis of a PWR nozzle gallery, in *Proceedings of ICAPP-2012*, 2012
3. X-5 Monte Carlo Team, MCNP—a general N-particle transport code, version 5, Los Alamos National Laboratory LA-UR-03-1987, 2003
4. D.G. Cepraga, G. Cambi, M. Frisoni, G.C. Panini, ANITA-2000, activation code package (manual—part I), ENEA Report ERG-FUS/TN-SIC TR 16/2000 Part I, 2000
5. D.G. Cepraga, G. Cambi, M. Frisoni, G.C. Panini, ANITA-2000, activation code package (validation—part II), ENEA Report ERG-FUS/TN-SIC TR 16/2000 Part II, 2000
6. T.T. Böhlen, F. Cerutti, M.P.W. Chin, A. Fassò, A. Ferrari, P.G. Ortega, A. Mairani, P.R. Sala, G. Smirnov, V. Vlachoudis, The FLUKA code: developments and challenges for high energy and medical applications. Nuclear Data Sheets **120**, 211–214 (2014)
7. A. Ferrari, P.R. Sala, A. Fasso, J. Ranft, FLUKA: a multi-particle transport code, CERN-2005-10, INFN/TC_05/11, SLAC-R-773, 2005
8. Y. Chen, U. Fischer, Rigorous MCNP based shutdown dose rate calculations: computational scheme, verification calculations and application to ITER. Fus. Eng. Des. **63**, 107–114 (2002)
9. A. Vaught, Introduction to Named Pipes, Linux Journal Issue #41, 1997
10. M. Snir, W. Gropp, S. Otto, S. Huss-Lederman et al., *MPI: the complete reference*, vol. 2 (MIT Press, Massachusetts, 1999)
11. G. Firpo, S. Frambati, M. Frignani, G. Gerra, Benchmarking and parallel scalability of MANCINTAP, a parallel high-performance tool for neutron activation analysis in complex 4D scenarios, in *SNA+MC 2013*, p. 04308, 2014